Pergamon

Bioorganic & Medicinal Chemistry, Vol. 5, No. 11, pp 2019–2027, 1997

PII: S0968-0896(97)00131-4
0968-0896/97 $17.00 + 0.00

Alkylation of a Catalytic Aspartate Group of the SIV Protease by an Epoxide Inhibitor

Patricia S. Caldera, Zhonghua Yu, Ronald M. A. Knegtel, Fiona McPhee, Alma L. Burlingame, Charles S. Craik, Irwin D. Kuntz and Paul R. Ortiz de Montellano*

Department of Pharmaceutical Chemistry, School of Pharmacy, University of California, San Francisco, CA 94143-0446, U.S.A.

Abstract—Specific irreversible inhibition of the SIV protease by FMOC-protected piperidine epoxide **1** involves alkylation of the protein. Tryptic digestion of the alkylated protein and mass spectrometric analysis of the peptides identify an active site aspartic acid (Asp-25) as the single residue that is alkylated. Computer modeling of **1** bound in the crystal structure of the SIV protease using DOCK 3.5 indicates that **1** has appropriate access to the active site. It is able to align in an orientation that allows a proton to be transferred to the epoxide from one of the catalytic aspartic acid groups in conjunction with nucleophilic attack on the epoxide of the carboxylate moiety of the second catalytic aspartic acid residue. Hydrophobic interactions are not optimal for this process due, in part, to the rigidity of the inhibitor ring system and the planar conformation of the amide. The combination of modeling with protein alkylation can provide insights into structural modifications of the inhibitor that may lead to improved inhibitory activity. © 1997 Elsevier Science Ltd.

Introduction

Simian immunodeficiency virus (SIV) is a retrovirus that is responsible for a disease in rhesus monkeys that resembles human AIDS.[1] Rhesus monkeys infected with the SIV virus provide an animal model for the testing of therapeutic agents that target the human immunodeficiency viruses (HIV-1 and HIV-2). Structural analysis shows that the active site of the SIV protease only differs from that of the HIV-1 protease in three of the 13 residues identified as the major contributors to substrate binding.[2] Furthermore, the active site of the SIV protease is identical to that of the HIV-2 protease with respect to all the 13 critical active site residues.

The crystal structures of the HIV-1 and HIV-2 proteases, and of a variant of the SIV (SIV S4H) protease, show remarkable similarities.[3] The crystal structure of the SIV S4H protease with a bound inhibitor shows the active site flaps fully closed, as is observed for the HIV-1 and HIV-2 proteases bound to peptidomimetic inhibitors.[4,5] A water molecule (H_2O-301) is also present and is hydrogen bonded between the flaps, as in the other HIV protease crystal structures.

Specific irreversible inhibition due to alkylation of the active site aspartic acid residues by the epoxide moieties in **1** and EPNP (Fig. 1) has been demonstrated for the HIV-1 protease by proteolysis of the inactivated enzyme and mass spectrometric sequencing of the peptides.[6] Similar specific irreversible inhibition by **1** is demonstrated here for the SIV S4H protease.

Previous studies of the irreversible inhibition of the SIV S4H protease by EPNP led to successful determination of the crystal structure of the protease with a single molecule of EPNP covalently bound to an active site aspartic acid residue.[3] Remarkably, this structure had similarities to the structures of HIV-1 and HIV-2 proteases with bound peptidomimetic inhibitors, including the fully closed position of the active site flaps. A single molecule of the inhibitor is bound per protease dimer.

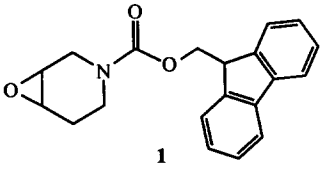

1

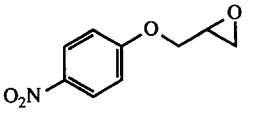

EPNP

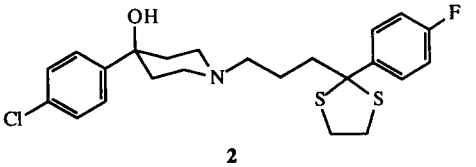

2

Figure 1. Structures of the irreversible inhibitors **1** and EPNP, and the reversible haloperidol-derived inhibitor **2**.

The present studies were intended to further our understanding of the mechanism of action of epoxide irreversible inhibitors. Compound **1** is a *cis*-epoxide and, as demonstrated by the mass spectrometric studies, shows a remarkably selective reactivity for the active site aspartic acids of the proteases. Structurally, the EPNP epoxide covalently bound to SIV S4H protease provides a possible model for the binding of epoxide **1** since both epoxides should act by a similar mechanism.

Molecular docking is a tool that can provide insight into the conformation of a protein–ligand complex, such as that of **1** with SIV, in the absence of experimental structural data. The DOCK program places rigid molecules in specified binding pockets in biological macromolecules by matching distances between ligand atoms with those between the centers of spheres[7,8] generated from the molecular surface of the protein.[9] Both ligands and protein are treated as rigid bodies in order to reduce the required amount of spatial sampling. Some ligand flexibility can be introduced, however, by docking a database of low energy ligand conformers instead of a single ligand structure. Scoring of the ligand orientations generated by DOCK is performed by a grid representation of the receptor contributions to the AMBER[10] inter-molecular energy.[11] Simplex rigid body minimization is applied for the refinement of the force field score and ligand orientation.[12] Although the formation of a covalent bond between the inhibitor and SIV protease cannot be simulated by molecular docking, modifications of atomic parameters for the active site residues can be used to accommodate the short distances implicit in covalent bonds.

Results

Enzyme inactivation

Compound **1** is an effective irreversible inhibitor of the HIV-1 protease[6] and, as shown here, similarly inactivates the SIV protease in a time dependent fashion. The $t_{1/2}$ value for inactivation is 240 min with a 100 μM inhibitor concentration of the inhibitor. The kinetic values for inactivation are K_{inact} = 770 μM and V_{inact} = 0.014 min^{-1}. These values are comparable to, though somewhat higher than, those found for inactivation of the HIV-1 protease by **1** (K_{inact} = 65 μM; V_{inact} = 0.009 min^{-1}; $t_{1/2}$ = 110 min)[6] and are better than those for inactivation of SIV protease by EPNP.[3]

Mass spectrometry

HPLC analysis of the SIV protease after complete inactivation by **1** demonstrates the presence to two peaks of comparable size (Fig. 2A). The first peak has the same retention time as the intact protease monomer and, indeed, has the same mass (Fig. 2B). The second peak shows a molecular mass of 11,120, which is 321 higher than the intact protease monomer (Fig. 2C). This difference in mass is exactly the molecular weight of **1**. Covalent binding thus occurs at only one of the two subunits of the fully inactivated dimer. Furthermore, proteolysis of the intact and modified monomers of the protease with pepsin reveals different peptide HPLC profiles for the alkylated and unalkylated proteins. Analysis of the HPLC peaks unique to the modified monomer by mass spectrometry and tandem mass spectrometry identify the sequence Val-Leu-Leu-Asp-Thr-Gly-Ala-Asp with **1** attached to the first aspartic acid residue (Fig. 3). This sequence, which corresponds to residues 22–29, shows that Asp-25 is the site of covalent modification. Alkylation of the aspartate is responsible for irreversible inactivation of the SIV protease.

Molecular modeling

Since **1** and EPNP are different structures a molecular modeling study provided some insight into the possible binding mode of **1**. A total of 491 low-energy conformers of **1** were generated by SYBYL. These structures were converted to a DOCK 3.5 database for use in molecular docking. The docked ligand orientations were analyzed to identify configurations suitable for the formation of a covalent bond between the enzyme and inhibitor. This requires the epoxide oxygen to be directed towards the proton shared between the catalytic aspartates, and positioning of one of the epoxide carbon atoms close to one of the aspartate carboxyl oxygen atoms.[3] A favorable force field score, chemically reasonable placement of the ligand in the binding site, and a low internal energy of the conformer are further requirements.

A configuration of the inhibitor that fulfilled all of the above mentioned criteria ranked 72nd among the docked conformers of **1** (Fig. 4). It has a force field score of −29.3 kcal/mol while the best docking solution has a score of −36.9 kcal/mol. Ligand orientations with better scores did not have the epoxide group placed near the catalytic aspartates suitably for a *trans*-addition and were therefore discarded. With an internal Tripos force field energy of 128.6 kcal/mol this conformer compares favorably with the internal energies observed for all 491 conformers, which ranged from 123.5 to 188.8 kcal/mol. The epoxide oxygen is at 1.9 Å from the Asp-25′ proton while carbon atoms 3 and 4 of the piperidine ring are at 1.4 and 1.6 Å, respectively, from the Asp-25 carboxyl oxygen atom. This conformation of the inhibitor places the epoxide oxygen in a favorable configuration to accept the proton shared between the two aspartates. In addition, it allows for a close approach of the Asp-25 carboxyl oxygen to carbon 3 of the piperidine ring to initiate the nucleophilic attack. Some suitable orientations with lower scores were also generated by DOCK but these were either similar to the one described above or represented a configuration unsuitable for *trans*-addition to the epoxide moiety.

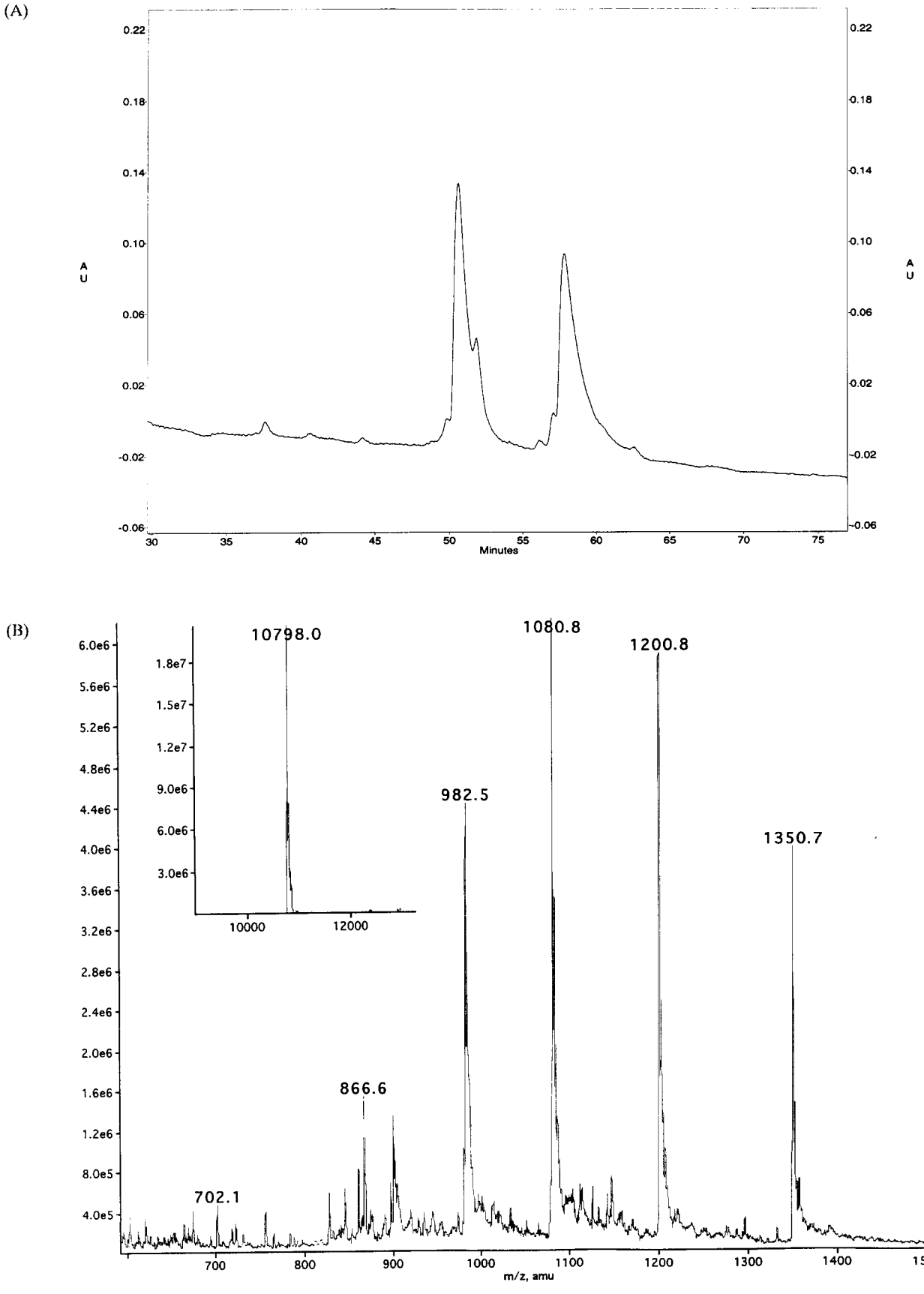

Figure 2. (A) HPLC profile of the SIV adduct with 1. Two major peaks of approximately equal size are observed with UV detection; (B) The molecular mass of the first peak, as calculated from the multiply charged ion peaks, is 10,798 (inset). This corresponds to the molecular ion of the native protease monomer (10,799 daltons); (C) (overleaf) The molecular mass of the second peak, as calculated from the ESIMS spectrum, is 11,120 (inset).

(C)

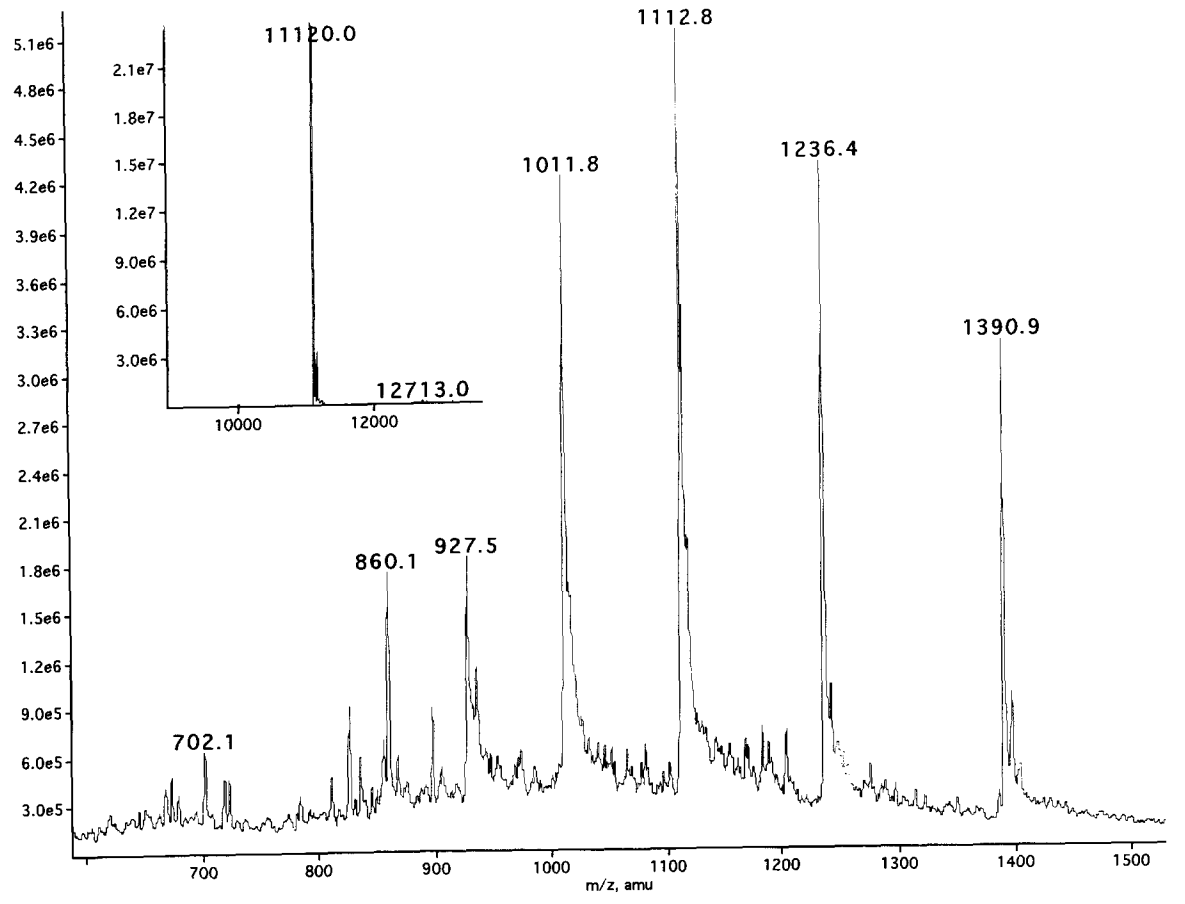

Figure 2. *continued.*

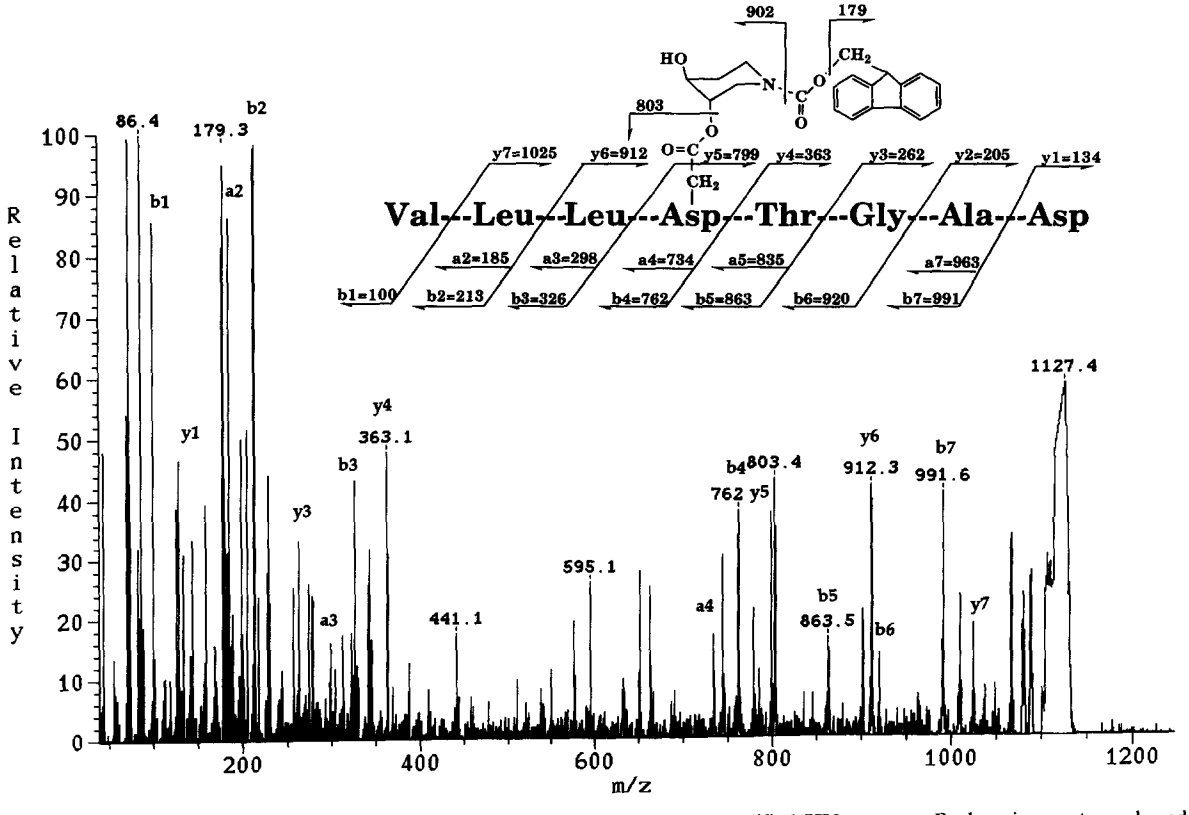

Figure 3. CID spectrum of the EPNP-modified peptide isolated after digestion of the modified SIV protease. Peak assignments are based on the nomenclature of Roepstorff and Fohlman[27] and Biemann.[28] The interpretation, shown on the panel above the spectrum, identifies Asp-25 as the site of covalent modification.

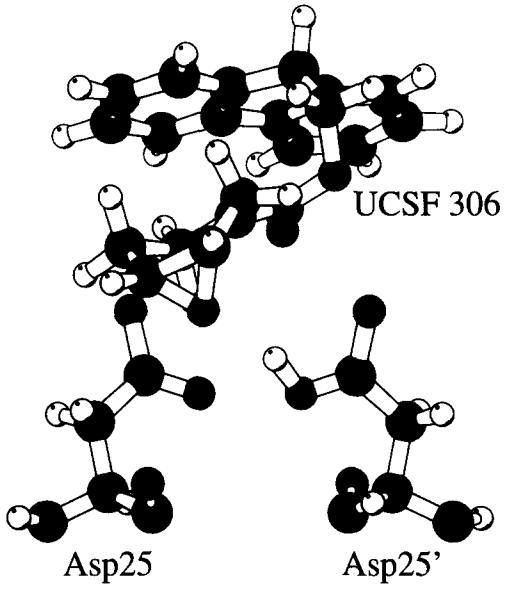

Figure 4. Stereo representation of the configuration near the catalytic aspartates of the docked complex between **1** and the SIV protease. The epoxide oxygen of **1** is positioned to accept a proton from Asp-25′. The Asp-25 carboxyl oxygen is sufficiently close for concurrent nucleophilic attack on a carbon of the epoxide ring.

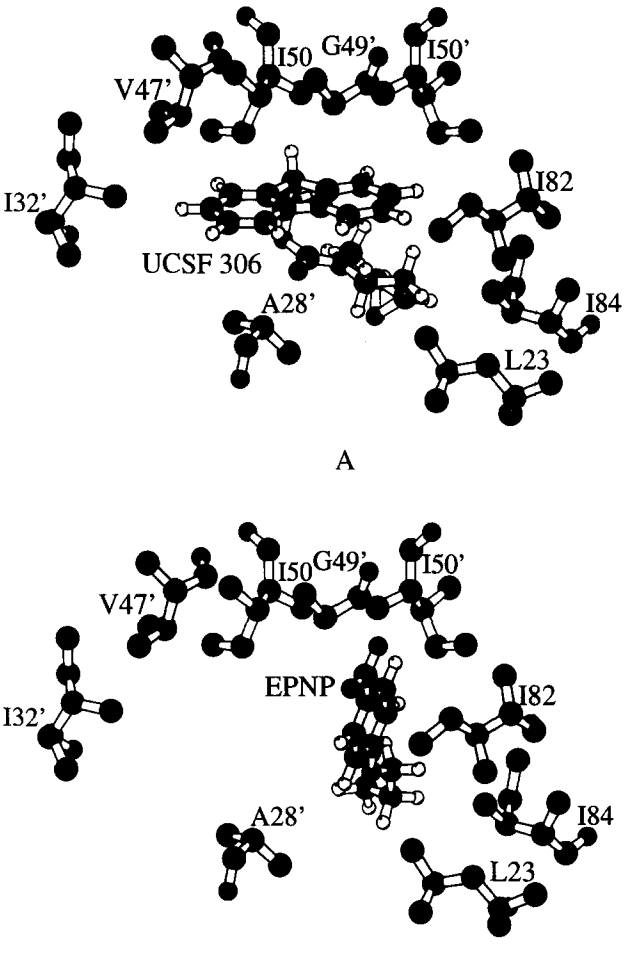

Figure 5. Hydrophobic residues of SIV protease (A) near the FMOC group of the docked structure of **1** and (B) in the crystal structure of the complex with EPNP (3). Protons of protein residues have been omitted for clarity. Since the FMOC-group of **1** is larger than the nitrophenoxy group of EPNP it is projected out of the binding pocket and partially exposed to the solvent in the docked conformation.

In the model, the FMOC moiety of the inhibitor is partially placed in a hydrophobic pocket formed by residues Leu-23, Ala-28, Gly-49, Ile-50, Pro-81, Ile-82 and Ile-84, with Pro-81 and Ile-84 making the closest contacts. Although it is difficult to predict how the formation of a covalent bond between Asp-25 and the inhibitor will affect the binding mode, the model derived by docking resembles the binding mode of EPNP. The nitrophenoxy group of EPNP as observed in its complex with the SIV protease, is oriented approximately parallel with the FMOC ring system (with a 40° angle between both planes) and has contacts with Leu-23, Ile-82 and Ile-84. Its phenyl ring approximately overlaps with one of the two phenyl rings which constitute the FMOC group. Due to the larger size of **1** compared to EPNP, however, the second benzyl moiety of the FMOC group is projected out of the binding pocket (see Fig. 5) exposing it to the solvent. Where **1** displays an entirely hydrophobic surface to the solvent, the nitro group of EPNP protrudes out of the binding pocket. No clear electrostatic interactions between the enzyme and inhibitor are observed in our model whereas the nitro group of EPNP was observed to contact the guanidinium group of Arg-8. Therefore, although **1** clearly allows for increased hydrophobic contact between the enzyme and inhibitor, some aspects of its binding may be considered less than optimal. In addition, the relatively rigid piperidine ring and planar amide group may conformationally restrict the inhibitor in acquiring optimal van der Waals' contacts with hydrophobic sites of the enzyme.

Discussion

The use of protease inhibitors in combination therapy with reverse transcriptase inhibitors has greatly improved the ability to block replication of the virus in cell culture and in a clinical setting. However, strains of the virus with mutations that convey resistance to the known protease and reverse transcriptase inhibitors have rapidly evolved. Resistance reflects loss of affinity for the inhibitors due to site specific mutations of the protease or reverse transcriptase. Irreversible inhibitors targeted to the catalytic reactive residues in the active site should be less susceptible to the development of resistance because inactivation should occur even if there is a decrease in the time-averaged occupancy of the active site by the inhibitor.

Inactivation of the SIV protease by **1**, as shown here, is mediated by exclusive alkylation of one of the two catalytic aspartic acid groups. The SIV protease is thus inactivated by **1** in the same manner as previously determined for inactivation of the HIV-1 protease by the same agent. HPLC (Fig. 2A) and mass spectrometric determination of the molecular mass of the alkylated protein (Fig. 2C) indicates that inactivation involves covalent binding of a single equivalent of **1** per protein dimer. The residue alkylated by the epoxide

moiety of **1** is unambiguously identified as Asp-25 by peptidic digestion of the inactivated (alkylated) protein and mass spectrometric characterization of the alkylated peptide (Fig. 3).

Alkylation of the protein presumably involves protonation of the epoxide oxygen by Asp-25′ with concomitant backside attack of the carboxylate anion of Asp-25 on the epoxide ring (Fig. 6). The reactivity of the epoxide must be appropriate for this reaction if it is to be an effective inactivating agent. Previous studies of the requirements for alkylation of the HIV protease aspartate groups have shown that a *cis*-1,2-disubstituted epoxide such as **1** has the appropriate reactivity.[6] Even in the presence of cysteine sulfhydryl groups, **1** has been shown to react preferentially with the two-aspartate motif of the HIV proteases.

Modeling studies suggest that the energetically favored docking of **1** resembles the binding mode observed for EPNP and SIV, specifically in the manner in which the aromatic ring systems are placed. The docking studies indicate that the epoxide oxygen is favorably positioned to accept the proton shared by the catalytic aspartates, and carbon 3 of the piperidine ring is located 1.3 Å away from the Asp-25 carboxylic oxygen and is thus positioned for the required nucleophilic addition step. The docking studies also show, however, that the rest of the structure of compound **1** exhibits an unfavorable placing of its large hydrophobic functionality by partially exposing it to the solvent. These features undoubtedly diminish the initial binding of the inhibitor to not only the SIV but also the HIV-1 and HIV-2 (unpublished data) proteases.

The present results indicate that the development of a more efficient irreversible inhibitor of the SIV and HIV proteases can be achieved by optimizing the interactions of the inhibitor with the protein while preserving the favorable reactivity and orientation of the epoxide moiety. Modifications to the structure to provide optimal hydrophobic interactions should increase the binding affinity of inhibitors such as **1** without compromising the specificity of the reaction.

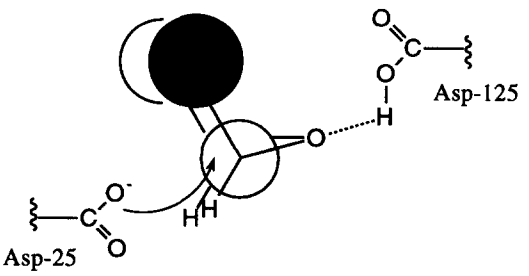

Figure 6. Mechanism proposed for specific alkylation of Asp-25 by a *cis*-disubstituted epoxide such as **1**. The alkylation is facilitated by protonation of the epoxide by the vicinal Asp-125 (i.e., Asp-25′).

Experimental

Materials and general methods

1,2-Epoxy-3-(*p*-nitrophenoxy)propane (EPNP) was supplied by Sigma (St Louis, MO). Compound **1** was synthesized and characterized as described elsewhere.[6] Mass spectra were obtained at the University of California San Francisco Mass Spectrometry Facility.

SIV Protease expression, purification, and assays

The expression and purification of SIV protease has been described.[13] The protein was purified to homogeneity and its concentration determined by active site titration using the peptidomimetic inhibitor U-85548, Val-Ser-Gln-Asn-Leu-ψ-[CH(OH)CH_2]-Val-Ile-Val, a gift of Dr A. Tomasselli (Upjohn Company, Kalamazoo, MI).[14] Fluorescence measurements were carried out on a Fluoroskan II (Labsystems Inc., Marlboro, MA). SIV protease was assayed against the fluorescent substrate, aminobenzoyl-Thr-Ile-Nle-Phe(*p*-NO_2)-Gln-Arg-NH_2, kindly provided by Dr Jorge P. Li (Sandoz Agro Inc., Palo Alto, CA). Stock solutions of substrate (1–10 mM) were freshly prepared in DMSO. The enzyme was assayed as previously described at pH 5.5 in 50 mM acetate buffer containing 1 M NaCl, 1 mM EDTA, and 1 mM DTT.[15]

Inactivation of the SIV protease

SIV PR (concentration ~50 μg/mL) was preincubated with 5 mM EPNP at ~25 °C in 250 mM sodium acetate buffer (pH 5.5) containing 0.5 M NaCl, 1 mM EDTA, 0.5 mM DTT, 5 mM EPNP, and 10% DMSO. For quantitation of the irreversible inactivation of SIV protease by compound **1**, SIV PR (30 μg/mL final concentration) was preincubated at 25 °C in 50 mM HEPES, pH 8.0, containing 1 M NaCl, 1 mM EDTA, 0.5 mM DTT, and 5% DMSO in the presence of a 20 μM–1.1 mM inhibitor concentration. Baseline measurements were carried out using 5% DMSO in the absence of inhibitors. At various times, aliquots were removed and assayed for activity. The SIV protease was assayed against the fluorescent substrate ABZ-TInLF(NO_2)-QR-NH_2 as previously described.[15] For calculation of the rates of inactivation, kinetic data were fit to a pseudo-first-order equation according to the formula $\ln(v_i/v_o) = -k_{obs}t$. From a plot of inactivation rates (k_{obs}) versus the square of the inhibitor concentration, k_{inact}, the inhibitor concentration resulting in half-maximal inactivation, and V_{inact}, the maximum inactivation rate, were calculated. In preparing the proteins for digestion and mass spectrometric work, the loss of activity was monitored by a UV assay using the peptide Arg-Val-nLeu-Phe-(*p*-NO_2)-Glu-Ala-nLeu-Ser-NH_2 (Bioserv, San Diego, CA). Aliquots of the protease–inhibitor complex were removed, and the protease activity was assessed by measuring the change in UV absorbance at

300 nm, the characteristic absorbance maximum of the substrate.

HPLC purification of the inhibited SIV protease

The inhibited enzyme was isolated by reverse phase HPLC on a C-4 column (4.6 mm × 250 mm, Vydac) using a 75-min gradient from 30 to 55% solvent B (acetonitrile containing 0.08% trifluoroacetic acid) against solvent A (water containing 0.1% trifluoroacetic acid). A flow rate of 1 mL/min was used and the effluent was monitored with a UV–vis detector. The enzyme fractions were collected and lyophilized for further characterization.

Protein molecular weight determination

The HPLC purified protein fractions were analyzed by electrospray ionization mass spectrometry on a PE Sciex API 300 mass spectrometer equipped with an electrospray ion source.[16] The samples were dissolved in an aqueous solvent (40% acetonitrile and 1% acetic acid) and 5 μL aliquots (approximately 10 pmol/μL) were injected into the mass spectrometer. The solvent system for batch mode electrospray contained 50% methanol and 1% acetic acid. The flow rate was 5 μL/min and the mass range was set at 400–2000 with a sweep rate of 7 s per scan. Approximately 10 scans were accumulated into one spectrum for better signal to noise ratio. The average molecular weight of each species was calculated based on the multiple charge nature of electrospray ionization.[17]

Enzymatic digestion

The HPLC fractions containing the modified protease were subjected to enzymatic digestion to determine the site of modification of the inhibitor. For tryptic digestion, the samples were dissolved in 20 μL 8 M urea, then diluted by adding 80 μL of 100 mM ammonium bicarbonate pH 8.3 to a final concentration of 80 mM NH_4HCO_3 and 1.6 M urea. Enzymes were then added to a concentration of ~4% of the sample. The digestion was carried out at 37 °C for 4 h but in some cases was continued overnight. For digestion by pepsin, the samples were first dissolved in 70% formic acid, then 20 volumes of 1 mM HCl containing pepsin were added to the sample. The ratio of protein to enzyme was about 50:1. The digestion was carried out at room temperature for 0.5 to 2 h and stopped by lyophilization or by injection onto a C-18 reverse-phase HPLC column.

Peptide molecular weight measurement

Molecular weights of the enzymatic peptides were determined by LC/ESIMS. These experiments were performed on the VG Platform mass spectrometer equipped with an ABI Model 140B HPLC system, using a microbore C-18 reverse-phase HPLC column (1 mm × 100 mm, ABI). A 50-min linear gradient from 2 to 52% solvent B was run at a flow rate of 50 μL/min. Solvent A was 0.1% formic acid in H_2O and solvent B was 0.05% formic acid in 10% isopropanol/90% ethanol. The mass spectrometer was set to a *m/z* range of 350–2100 with a sweep speed of 5 s/scan. Subsequent isolation of the modified peptides was carried out using an analytical C-18 HPLC column (Vydac 4.6 mm × 250 mm) employing conditions as described above.

Tandem mass spectrometry

Selected peptides were subjected to high energy CID analysis on a Kratos Concept IIHH 4-sector tandem mass spectrometer. Samples were introduced into the instrument through a flow probe with a flow rate of 3 μL/min. The delivery solvent contained 5% acetonitrile, 2% thioglycerol, and 0.1% trifluoroacetic acid in H_2O. The precursor ion was subjected to CID process in the collision cell at a helium gas pressure which resulted in an attenuation of its abundance to 30% of the original value. The resulting CID spectra were recorded on a rapid scanning multichannel array detector.[18,19]

Molecular modeling

Coordinates of the molecular structure of **1** were created using SYBYL V6.2 (Tripos, St Louis, MO). Two structures of **1** were generated with the epoxide moiety placed either above or underneath carbon positions 3 and 4 of the piperidine ring and Gasteiger–Marsili charges[20] were calculated for both forms. A conformer database was generated using the multisearch option in SYBYL which generates and minimizes random conformations of a given molecule. The TRIPOS force field[21] was used with a distance dependent dielectric constant ($\varepsilon = r$). The multisearch protocol allows for rotations around the amide bond in **1**. The epoxide moiety can therefore be rotated to positions above and below carbon atoms 4 and 5 of the piperidine ring, generating all four possible positions of the epoxide oxygen atom.

The conformers of **1** were pooled and converted to DOCK 3.5 database format for use in molecular docking with DOCK 3.5. The structure at 2.4 Å resolution of the SIV protease covalently bound to 1,2-epoxy-3-(*p*-nitrophenoxy) propane (EPNP)[3] was obtained from the protein data bank (PDB, entry 2sam). Since in the EPNP-bound form the side-chain conformations of Asp-25 in both monomers differ from those in the unliganded protein, the values of the 1 and 2 dihedral angles of both aspartates were set to those observed in the unliganded HIV protease structure[22] determined at 2.7 Å resolution (PDB entry 3phv). Protons were added to the SIV protease structure including the carboxyl group of Asp-25′ in the second monomer.

In order for a covalent link to form between the inhibitor and the enzyme, the epoxide should be favorably positioned with respect to the catalytic aspartates.[3] While the proton shared between the two aspartates is donated to the epoxide oxygen, the aspartate carboxyl oxygen attacks a carbon of the epoxide group in order to establish the new covalent bond. For the purpose of simulating such a reaction by molecular docking, the atoms of the epoxide moiety and the catalytic aspartates should be able to approach each other closely. Therefore the repulsive portion of the force field potentials of the carboxyl oxygens of Asp-25 in both monomers and of the proton shared between them was set to zero in the scoring grids used by DOCK 3.5.[23] In addition, the repulsive part of the force field potential of all atoms beyond the N_ε atom of the Arg-8 side-chain was removed. This residue interacts with the EPNP nitrophenoxy group in the adduct with the SIV protease[3] and could interfere with successful docking of the larger **1**.

Spheres were generated using SPHGEN[7] and edited to remove spheres remote from the binding site, yielding a total of 53 spheres. Two spheres located near the catalytic aspartates were labeled as critical spheres.[24] In the DOCK 3.5 implementation, the use of critical spheres implies that at least one of these two spheres is used in all matchings of internal inhibitor distances with inter-sphere distances. This results in a focusing of the spatial sampling to orientations close to the catalytic aspartates. Force field scoring grids were generated using a modified version of the CHEMGRID program[11,23] in order to allow for the removal of repulsive interactions between the inhibitor and the catalytic aspartates. For the enzyme, the AMBER united-atom force field[10] was used while for the inhibitor the all-atom AMBER force field[25] was applied. For docking, a distance-matching tolerance of 1 Å and bin sizes[8] of 0.5 Å with 0.2 Å overlap were used. Simplex minimization of ligand orientations[12] required a maximum of 500 iterations to reach convergence within 0.2 kcal/mol. Figures were created using MOLSCRIPT.[26]

Acknowledgements

The work reported here was supported by National Institutes of Health grant GM39552, NIH NCRR Biomedical Research Technology Program Grant RR01614, National Institute of Environmental Health Sciences Grant ES04705, and National Science Foundation Grant DIR 8700766. F.M. was a recipient of an AmFAR Fellowship, award number 70361-14-RF. R.M.A.K. acknowledges financial support from the Netherlands Organization for Scientific Research (NWO). We thank Fisons/VG for the loan of the platform electrospray mass spectrometer and Tripos for an academic software license.

References

1. Kestler, H.; Kodama, T.; Ringler, D.; Marthas, M.; Pedersen, N.; Lackner, A.; Regier, D.; Sehgal, P.; Daniel, M.; King, N.; Desrosiers, R. *Science* **1990**, *220*, 671.

2. Miller, M.; Jaskolski M.; Rao, J. K.; Leis, J.; Wlodawer, A. *Nature (London)* **1989**, *337*, 576.

3. Rose, R. B.; Rosé, J. R.; Salto, R.; Craik, C. S.; Stroud, R. M. *Biochemistry* **1993**, *32*, 12498.

4. Swain, A. L.; Miller M. M.; Green, J.; Rich, D. L.; Schneider, J.; Kent, S. B. H.; Wlodawer, A. *Proc. Natl. Acad. Sci. U.S.A.* **1990**, *87*, 8805.

5. Mulichak, A. M.; Hui, J. O.; Tomasselli, A. G.; Heinrikson, R. L.; Curry, K. A.; Tomich, C.; Thaisrivong, S.; Sawyer, T. K.; Watenpaugh, K. D. *J. Biol. Chem.* **1993**, *268*, 13103.

6. Yu, Z.; Caldera, P.; McPhee, F.; De Voss, J. J.; Jones, P. R.; Burlingame, A.; Kuntz, I. D.; Craik, C. S.; Ortiz de Montellano, P. R. *J. Am. Chem. Soc.* **1996**, *118*, 5846.

7. Kuntz, I. D.; Blaney, J. M.; Oatley, S. L.; Langridge, R.; Ferrin, T. E. *J. Mol. Biol.* **1982**, *161*, 269.

8. Schoichet, B. K.; Bodian, D. L.; Kuntz, I. D. *J. Comput. Chem.* **1992**, *13*, 380.

9. Connolly, M. L. *J. Appl. Cryst.* **1983**, *16*, 54.

10. Weiner, S. J.; Kollman, P. A.; Case, D. A.; Singh, U. C.; Ghio, C.; Alagona, G.; Profeta, S.; Weiner, P. A. *J. Am. Chem. Soc.* **1984**, *106*, 765.

11. Meng, E. C.; Schoichet, B. K.; Kuntz, I. D. *J. Comp. Chem.* **1992**, *13*, 505.

12. Meng, E. C.; Gschwend, D. A.; Blaney, J. M.; Kuntz, I. D. *Proteins* **1993**, *17*, 266.

13. Rosé, J.; Salto, R.; Craik, C. S. *J. Biol. Chem.* **1993**, *268*, 11939.

14. Tomasselli, A. G.; Hui, J. O.; Sawyer, T. K.; Staples, D. J.; Bannow, C.; Reardon, I. M.; Howe, W. J.; DeCamp, D. L.; Craik, C. S.; Heinrikson, R. L. *J. Biol. Chem.* **1990**, *265*, 14675.

15. Toth, M.; Marshal, G. *Int. J. Peptide Res.* **1990**, *36*, 544.

16. Fenn, J. B.; Mann, M.; Meng, C. K.; Wong, S. F.; Whitehouse, C. M. *Science* **1989**, *246*, 64.

17. Carr, S. A.; Burlingame, A. L. In *Mass Spectrometry in the Biological Sciences*; Burlingame, A. L.; Carr, S. A., Eds. Humana: Totowa, 1996; pp 546–553.

18. Walls, F. C.; Hall, S. C.; Medzihradsky, K. F.; Yu, Z., Burlingame, A. L.; Evans, S.; Hoffman, A. D.; Buchanan, R.; Glover, S. In *Proceedings of the 41st ASMS Conference on Mass Spectrometry and Allied Topics*; San Francisco, 1994; p 937.

19. Burlingame, A. L. In *Biological Mass Spectrometry: Present and Future*; Matsuo, T.; Caprioli, R. M.; Gross, M. L.; Seyama, Y., Eds.; John Wiley: New York, 1994; pp 147–164.

20. Gasteiger, J.; Marsili, M. *Tetrahedron Lett.* **1980**, *36*, 3219.

21. Clark, M.; Cramer III, R. D.; van Opdenbosch, N. *J. Comp. Chem.* **1989**, *10*, 982.

22. Lapatto, R.; Blundell, T.; Hemmings, A.; Overington, J.; Wilderspin, A.; Wood, S.; Merson, J. R.; Whittle, P. J.; Danley, D. E.; Geoghegan, K. F.; Hawrylik, S. J.; Lee, S. E.; Scheld, K. G.; Hobart, P. M. *Nature (London)* **1989**, *342*, 299.

23. Knegtel, R. M. A.; Kuntz, I. D.; Oshiro, C. M. *J. Mol. Biol.* **1997**, *266*, 424.

24. DesJarlais, R. L.; Dixon, J. S. *J. Comp.-Aided Design* **1994**, *8*, 231.

25. Weiner, S. J.; Kollman, P. A.; Hguyen, D. T.; Case, D. A. *J. Comp. Chem.* **1986**, *7*, 230.

26. Kraulis, P. J. *J. Appl. Cryst.* **1991**, *24*, 946.

27. Roestorff, P.; Fohlman, J. *J. Biomed. Mass Spectrom.* **1984**, *11*, 601.

28. Biemann, K. *Methods Enzymol.* **1990**, *193*, 886.

(*Received in U.S.A.* 17 *February* 1997; *accepted* 9 *June* 1997)